the plant journal

SEB SOCIETY FOR EXPERIMENTAL BIOLOGY

The Plant Journal (2024) **119**, 3000–3014 doi: 10.1111/tpj.16967

Nonphotochemical quenching kinetics GWAS in sorghum identifies genes that may play conserved roles in maize and *Arabidopsis thaliana* photoprotection

Seema Sahay[1,2,†], Nikee Shrestha[2,3,†], Henrique Moura Dias[2,3,4], Ravi V. Mural[2,3,‡], Marcin Grzybowski[2,3,5], James C. Schnable[2,3,*] and Katarzyna Głowacka[1,2,6,*]

[1]*Department of Biochemistry, University of Nebraska-Lincoln, Lincoln, Nebraska, USA,*
[2]*Center for Plant Science Innovation, University of Nebraska-Lincoln, Lincoln, Nebraska, USA,*
[3]*Department of Agronomy and Horticulture, University of Nebraska-Lincoln, Lincoln, Nebraska, USA,*
[4]*Departamento de Botânica, Instituto de Biociências, Universidade de São Paulo, São Paulo, SP, Brazil,*
[5]*Faculty of Biology, University of Warsaw, Warsaw, Poland, and*
[6]*Institute of Plant Genetics, Polish Academy of Sciences, Poznan 60-479, Poland*

Received 16 November 2023; revised 28 May 2024; accepted 23 July 2024; published online 10 August 2024.
*For correspondence (e-mail schnable@unl.edu and kglowacka2@unl.edu).
†These authors contributed equally to this work.
‡Present address: Department of Agronomy, Horticulture, and Plant Science, South Dakota State University, Brookings, South Dakota, USA

SUMMARY

Photosynthetic organisms must cope with rapid fluctuations in light intensity. Nonphotochemical quenching (NPQ) enables the dissipation of excess light energy as heat under high light conditions, whereas its relaxation under low light maximizes photosynthetic productivity. We quantified variation in NPQ kinetics across a large sorghum (*Sorghum bicolor*) association panel in four environments, uncovering significant genetic control for NPQ. A genome-wide association study (GWAS) confidently identified three unique regions in the sorghum genome associated with NPQ and suggestive associations in an additional 61 regions. We detected strong signals from the sorghum ortholog of *Arabidopsis thaliana Suppressor Of Variegation 3* (*SVR3*) involved in plastid–nucleus signaling. By integrating GWAS results for NPQ across maize (*Zea mays*) and sorghum-association panels, we identified a second gene, *Non-yellowing 1* (*NYE1*), originally studied by Gregor Mendel in pea (*Pisum sativum*) and involved in the degradation of photosynthetic pigments in light-harvesting complexes. Analysis of *nye1* insertion alleles in *A. thaliana* confirmed the effect of this gene on NPQ kinetics in eudicots. We extended our comparative genomics GWAS framework across the entire maize and sorghum genomes, identifying four additional loci involved in NPQ kinetics. These results provide a baseline for increasing the accuracy and speed of candidate gene identification for GWAS in species with high linkage disequilibrium.

Keywords: nonphotochemical quenching, association mapping, comparative genomics, sorghum, maize.

INTRODUCTION

The leaves of plants grown under field conditions experience rapid fluctuations in the quantity of photosynthetically active light reaching their surface, resulting from both intermittent clouds passing in front of the sun and moving shadows caused by the wind blowing through leaf canopies (Burgess et al., 2016; Tang et al., 1988). In the absence of buffering mechanisms, rapid increases in light intensity can produce singlet oxygen and other reactive oxygen species (ROS) that can damage both the photosystems and other proteins throughout the cell (Muller et al., 2001). Plants have evolved several mechanisms to safely dissipate excess energy absorbed by the photosynthetic apparatus as heat, minimizing the formation of damaging ROS due to changes in light intensity. These mechanisms are collectively known as nonphotochemical quenching (NPQ). In discussions of NPQ below, we focus specifically on two components of NPQ: energy-dependent quenching (qE) and zeaxanthin-dependent quenching (qZ). qE is energy-dependent quenching that relaxes in less than 1 min—and is, therefore, the mechanism that responds most rapidly to changes in light intensity—whereas qZ has a slower relaxation time typically of 10 to 15 minutes (Muller et al., 2001). Genes encoding several proteins

involved in NPQ have been identified through forward genetic screens, including *PHOTOSYSTEM II SUBUNIT S* (*PSBS*), also named *NPQ4* based on the corresponding mutant (Li et al., 2000), *VIOLAXANTHIN DE-EPOXIDASE 1* (*VDE1*; or *NPQ1*), and *ZEAXANTHIN EPOXIDASE* (*ZEP*; or *NPQ2*) (Niyogi et al., 1998).

The kinetics of NPQ induction and relaxation reflect a core fitness trade-off for plants. Failure to induce NPQ rapidly enough or the inability to reach sufficient maximum values under high light conditions exposes plants to the risk of substantial damage and diminished photosynthetic productivity due to photoinhibition. However, NPQ induction beyond the levels necessary to protect plants from damage leads to the wasteful dissipation of photosynthetic energy as heat and reduced productivity, as does an insufficiently rapid drop in NPQ when light intensity declines (Kromdijk et al., 2016). Optimal and maximal values for NPQ induction and relaxation likely vary depending on both the external environment (e.g., frequency and type of cloud cover or maximum light intensity during the growing season) and properties of plant canopy architecture (Burgess et al., 2016; Kaiser et al., 2018; Pearcy, 1990; Tang et al., 1988). Whereas natural selection has shaped the response of plants to fluctuating light intensities over hundreds of millions of years, key crops have been under selection for performance in the artificial environments of agricultural fields for only thousands of years and have experienced selection for performance at modern planting densities that have profoundly reshaped crop and canopy architectures for only decades. As a result, the kinetics of NPQ in major crops may not be optimized for current growing environments (Zhu et al., 2004). Transgenic interventions to alter NPQ kinetics have achieved increases of 14–20% in dry biomass accumulation in tobacco (*Nicotiana tabacum*) plants grown under field conditions (Kromdijk et al., 2016) and significant increases in soybean (*Glycine max*) yields in one of two environments tested (De Souza et al., 2022).

Both crops and wild species exhibit substantial natural variation in NPQ (Gamba et al., 2022; Jung & Niyogi, 2009; Rungrat et al., 2019; Wei et al., 2022). A study of the maximum NPQ induction in rice (*Oryza sativa*) identified 33 loci, including the rice ortholog of *PSBS* (Wang et al., 2017). In soybean, a study of variation in the epoxidation state of the xanthophyll pigments, a key component of NPQ identified 15 loci, including one proximal to the soybean ortholog of *VDE* (Herritt et al., 2016). A genome-wide association study (GWAS) conducted in *Arabidopsis thaliana* (*A. thaliana*) identified 15 loci associated with variation in NPQ induction, maximum value, or relaxation, including one that co-localized with the previously characterized *PSBS* (Rungrat et al., 2019). *Arabidopsis thaliana*, rice, and soybean are all C_3 plants. A recent GWAS in maize (*Zea mays*), a C_4 plant identified 18 confident associated regions with different traits describing the kinetics of NPQ induction, maximum value, or relaxation, including a signal associated with the maize ortholog of *PSBS*. In six cases, insertion mutants in the *A. thaliana* orthologs of candidate genes adjacent to maize GWAS hits produced similar alterations in NPQ kinetics to those observed in maize (Sahay et al., 2023).

Here, we sought to identify genetic loci associated with variation in NPQ kinetics across a widely characterized and recently re-sequenced sorghum-association panel (*Sorghum bicolor*) (Boatwright et al., 2022; Casa et al., 2008; Mural et al., 2021), a drought-tolerant and nitrogen-use-efficient relative of maize that is widely grown as a staple crop in sub-Saharan Africa and South Asia. We identified several significant NPQ trait-associated loci including the sorghum ortholog of a gene previously reported in maize and *A. thaliana* (Sahay et al., 2023) and signal from sorghum and maize orthologs of *Non-yellowing 1* (*NYE1*). The quantification of the photosynthesis-related pigments confirmed the *NYE1* allelic effect of chlorophyll content. Multiple insertion alleles of *Nye1* exhibit impaired NPQ in *A. thaliana*, consistent with the maize and sorghum phenotypes. Collectively, these results begin to address the historically limited characterization of natural variation NPQ among C_4 species and support a core set of existing functional proteins playing conserved roles in determining NPQ kinetics across angiosperms.

RESULTS

Genetic variation of NPQ kinetics across different environments

We observed substantial variation in nine traits describing NPQ kinetics (Table 1) in a population of 339 sorghum genotypes (Data S1) grown under low-nitrogen (LN) conditions in 2020 (Figure 1; Figure S1). The LN treatment was sufficient to decrease sorghum grain yield by 48% relative to high-nitrogen (HN) controls. Other traits measured in the same field experiment, such as flag leaf width and length, also showed significant differences between treatments (Grzybowski et al., 2022). However, we did not observe consistent population-level responses of NPQ kinetics to nitrogen treatment across the 2 years of the experiment (Figure S2; Data S2). Correlations in observed NPQ kinetic values for the same genotypes measured across different years or under different nitrogen treatments were typically low. The correlation in observed NPQ kinetics between the same treatments in different years were lower than the correlations in NPQ kinetics between different treatments in the same year, suggesting environmental factors other than nitrogen availability play a greater role in shaping variation in NPQ (Figure S3; Data S2). The average within-environment heritability of NPQ kinetic traits was modestly lower in this sorghum experiment than previously reported for maize traits

Table 1 Descriptions of nonphotochemical quenching (NPQ) kinetic traits investigated in this paper

Kinetics Type	Kinetics Attributes	Trait Abbreviation Name	Trait Full Name	Trait Description
NPQ induction in light	Rate	$NPQslope_{lightH}$	Initial slope of NPQ in light	How fast NPQ is induced under high light. Estimated from a hyperbolic (H) curve fit to the different measurements of NPQ collected during the 10-min light treatment
		$NPQrate\ constant_{light}$	Rate constant of NPQ in light	Estimate of the rate at which NPQ reaches 63% of its final maximum potential value after being exposed to high light (min^{-1}), calculated from exponential function
	Steady state	$NPQasymptote_{lightH}$	Asymptote of NPQ in light	The maximum potential value NPQ would reach under prolonged high light. Estimated from a hyperbolic (H) curve fit to the different measurements of NPQ collected during the 10-minute light treatment
		NPQ_{max}	Maximum NPQ	The highest of NPQ during the 10-minute light treatment.
NPQ relaxation in light	N/A	$NPQstart_{darkH}$	Initial NPQ in the dark	The NPQ value at the transition point between high light and dark treatments. Estimated from a curve fit to the different measurements of NPQ collected during the 10-minute dark treatment.
	Rate	$NPQslope_{darkH}$	Initial slope of NPQ in dark	How fast NPQ relaxes once the lights are turned off. Estimated from a curve fit to the different measurements of NPQ collected during the 10-minute dark treatment
		$NPQrate\ constant_{dark}$	Rate constant of NPQ in dark	Estimate of the rate at which NPQ reaches 63% of its final minimum potential value after the end of illumination (min^{-1}), calculated from exponential function
	Range	$NPQamplitude_{darkH}$	NPQ amplitude in dark	Size of the change between estimated maximum NPQ induction and maximum post-induction NPQ relaxation, calculated from hyperbolic (H) fit
	Steady state	$NPQresidual_{dark}$	Residual of NPQ in dark	The amount of potential NPQ relaxation beyond that which occurs during the 10-min dark treatment, calculated from exponential function
		NPQ_{end}	Minimum NPQ in dark	Remaining NPQ still present after 10-min in the dark

(Table 2). Given the lack of clear response to nitrogen supply, we focused on measurements of NPQ kinetics from the LN conditions from 2020, as traits exhibited the higher average heritability in this environment ($H^2 = 0.50$) than the other three from which data were collected ($H^2 = 0.42$, 0.40 and 0.35, Table 2).

Genome wide association identifies significant signals for NPQ

A set of three significant marker–trait associations for two NPQ-related traits were identified at a confident threshold of ≥0.2 resampling model inclusion probability (RMIP) in a FarmCPU GWAS with resampling analysis conducted with 4.4 million resequencing derived markers (Figure 2a; Data S3). An additional 66 marker–trait associations exhibited RMIP values between the confident (RMIP ≥0.2) and suggestive value (RMIP ≥0.05). In some cases, the same genetic markers were identified across multiple NPQ kinetic traits and, as a result, the 69 marker–trait associations (MTAs) identified with RMIP ≥0.05 (3 RMIP ≥0.2 and 66 0.2 > RMIP ≥0.05) correspond to 64 unique genetic markers. We identified fewer significant associations in the analysis of NPQ kinetics traits scored in the three environments with lower heritability (Figure S4; Data S3).

The most stable signal in the GWAS analysis of the low nitrogen treatment experiment in 2020 came from a marker located at position 16 356 388 on sorghum chromosome 4 (RMIP = 0.44). This marker is 1.4 kb upstream from Sobic.004G128900 (Figure 2b) and more than 48 kb from the next closest gene (Figure S5). Sorghum genotypes homozygous for the minor allele at this locus exhibited more rapid induction of NPQ and higher maximum NPQ kinetics after 10 min under high-light conditions, but slower relaxation of NPQ under dark conditions than genotypes homozygous for the major allele (Figure 2c; Data S1). Sobic.004G128900 has 78.4% protein similarity with and is identified via InParanoid as the sole sorghum ortholog of the single-copy *A. thaliana* gene *Suppressor Of Variegation 3* (*SVR3*, At5g13650) (Goodstein et al., 2012). *SVR3* encodes a putative chloroplast translation elongation factor (Liu et al., 2010). We also observed significant differences between the values of NPQ at the end of the assay in dark (NPQ_{end}) for genotypes homozygous for the two possible alleles at marker position 16 356 388 on sorghum chromosome 4 under LN conditions in both 2020 and 2021 ($P < 0.001$ and $P = 0.03$), but not in the HN treatment in either year (Figure 2d; Data S2).

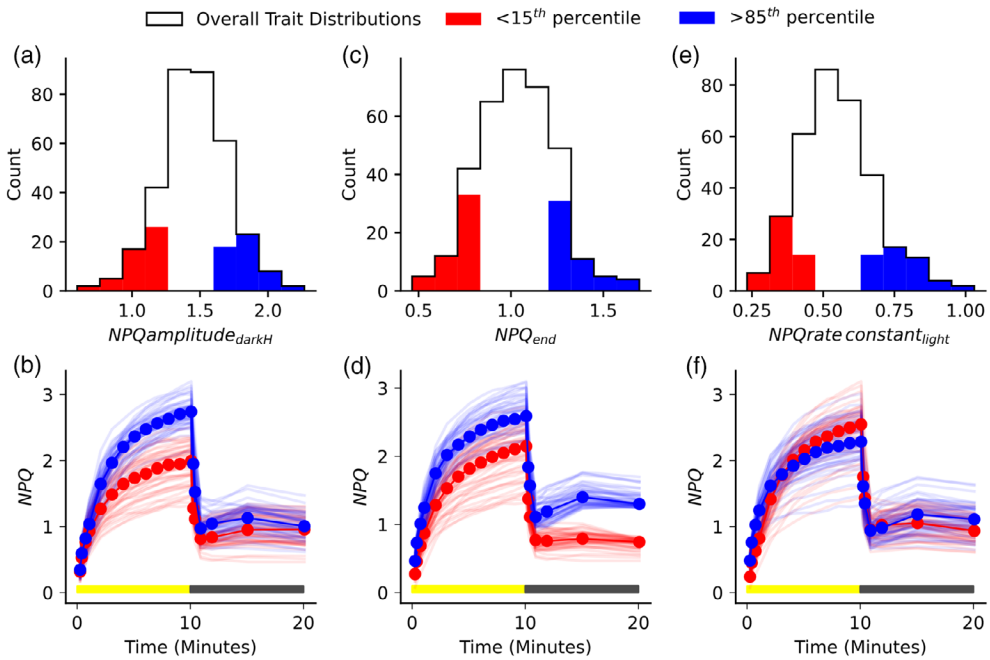

Figure 1. Patterns of NPQ kinetics associated with phenotypic extremes for three selected NPQ kinetics traits.
(a) Distribution of observed values for $NPQamplitude_{darkH}$ among the genotypes of the sorghum association panel grown in Lincoln, Nebraska, USA, in the summer of 2020 under low-nitrogen (LN) conditions ($n = 339$ sorghum genotypes).
(b) Genotype-specific patterns of NPQ induction and relaxation for the 15% of sorghum genotypes with the lowest $NPQamplitude_{darkH}$ scores (light red lines) and the 15% of sorghum genotypes with the highest $NPQamplitude_{darkH}$ scores (light blue lines). Median NPQ response among sorghum genotypes with the lowest and highest $NPQamplitude_{darkH}$ shown in solid red and blue, respectively.
(c) Distribution of observed values for NPQ_{end} among the same set of sorghum lines shown in a ($n = 339$ sorghum genotypes).
(d) Genotype-specific and median NPQ induction and relaxation curves for sorghum genotypes at both extremes of the distribution for NPQ_{end}, presented as described in (b).
(e) Distribution of observed values for $NPQrate\ constant_{light}$ among the same set of sorghum lines shown in (a). One genotype with median $NPQrate\ constant_{light} > 1.5$ was excluded to improve figure readability ($n = 338$ sorghum genotypes).
(f) Genotype-specific and median NPQ induction and relaxation curves for sorghum genotypes at both extremes of the distribution for $NPQrate\ \_constant_{light}$, presented as described in (b). Data used to produce this figure are given in Data S1.

Table 2 Heritability of nonphotochemical quenching (NPQ) traits in sorghum and maize

	Sorghum H^2				Maize H^2	
Trait	LN2020	LN2021	HN2020	HN2021	2020	2021
$NPQslope_{lightH}$	0.43	0.37	0.39	0.33	0.60	0.59
$NPQrate\ constant_{light}$	0.51	0.34	0.44	0.16	0.60	0.60
$NPQasymptote_{lightH}$	0.54	0.40	0.44	0.48	0.56	0.50
$NPQstart_{darkH}$	0.46	0.27	0.39	0.46	0.55	0.51
$NPQslope_{darkH}$	0.55	0.49	0.30	0.41	0.62	0.61
$NPQrate\ constant_{dark}$	0.51	0.47	0.37	0.34	0.63	0.54
$NPQamplitude_{darkH}$	0.44	0.29	0.42	0.40	0.56	0.50
$NPQresidual_{dark}$	0.54	0.26	0.51	0.51	0.49	0.45
NPQ_{end}	0.53	0.24	0.50	0.49	0.53	0.48
Average	0.50	0.35	0.42	0.40	0.57	0.53

HN, High nitrogen condition; LN, Low nitrogen condition.

The second most stable signal was located at position 56 606 003 (RMIP = 0.27) on sorghum chromosome 4. We were unable to locate any genes previously linked to variation in NPQ within 500 kb of this hit, suggesting this hit may correspond to variation in a currently uncharacterized gene or the true causal gene may be located more than 500 kb away from the signal although we cannot rule out the possibility that this signal may represent a false positive association.

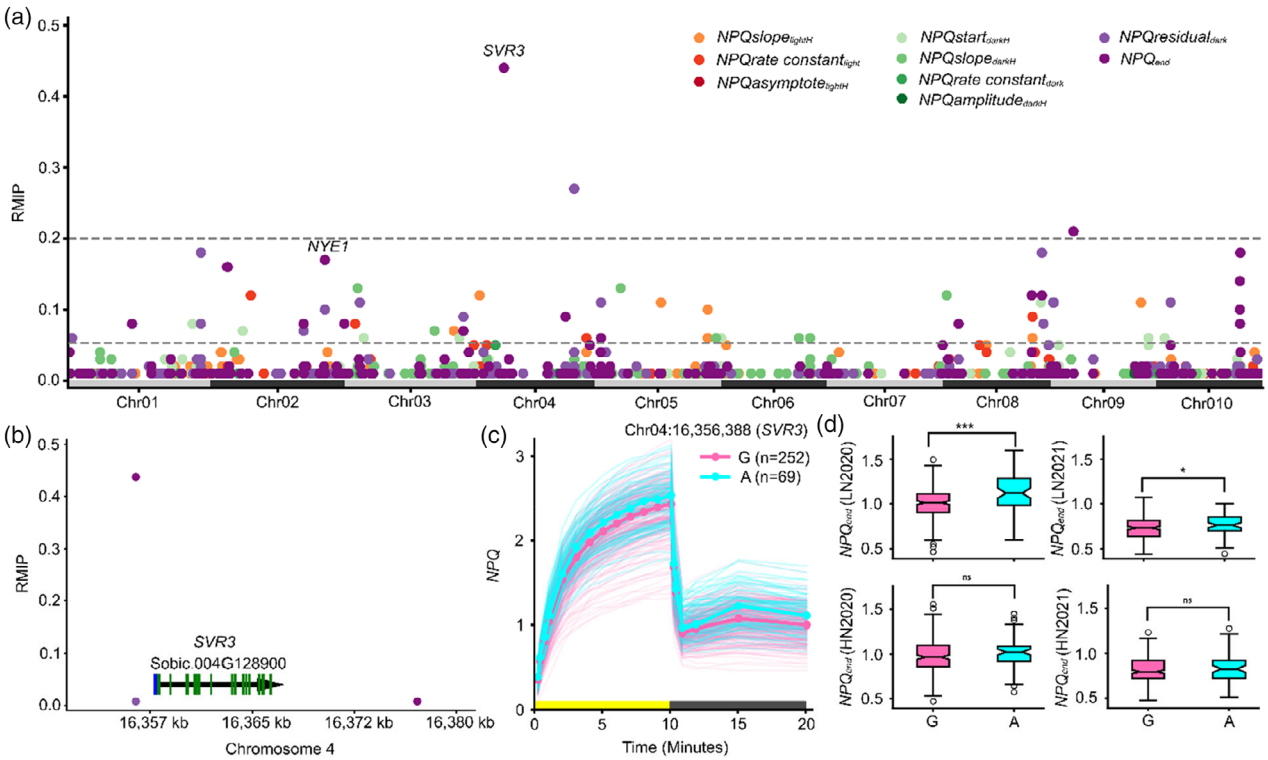

Figure 2. Results of genome-wide associations for NPQ kinetic traits in sorghum.
(a) Resampling model inclusion probabilities (RMIPs) for genetic markers linked to variation in 9 sorghum NPQ traits (Table 1) measured in the sorghum association panel grown under low-nitrogen conditions in the summer of 2020. The two dashed horizontal gray lines are drawn at a confident RMIP threshold of 0.2 and a suggestive RMIP threshold of 0.05. The patterns of change in NPQ response curves associated with each of these nine traits are shown in Figure S1.
(b) Zoomed in view of trait-associated SNPs from panel (a) for a 30-kb region including the highest RMIP marker located at 16 356 388 on sorghum chromosome 4. Green boxes indicate exons and blue boxes indicate untranslated regions of exons of a gene, 1.4 kb upstream from the SNP.
(c) NPQ response curves for sorghum genotypes homozygous for either the major allele (G) or the minor allele (A) Chr04:16 356 388.
(d) NPQ_{end} values measured under low-nitrogen conditions (LN2020 and LN2021) and high-nitrogen conditions (HN2020 and HN2021) for sorghum genotypes homozygous for either G or A at Chr04:16 356 388. In panel (d) colored boxes indicate the range from the 25th–75th percentile of values, black lines with notches within the colored boxes indicate the median value, whiskers indicate the most extreme values within 1.5× the interquartile range and white circles with black outlines indicate the values of datapoints outside that range. For each comparison in (d), $n = 252$ sorghum genotypes for the G allele and $n = 69$ sorghum genotypes for the A allele. $^{*}P < 0.05$, $^{***}P < 0.001$, n.s., not significant (two-tailed *t*-test). Data used to produce this figure are given in Data S1, S2, and S3.

Comparative GWAS identifies a role of *Non-yellowing1* (*NYE1*) in controlling NPQ in sorghum, maize, and *A. thaliana*

Two suggestive trait-associated genetic markers on sorghum chromosome 2, separated by 21 kb, were associated with traits describing relaxation of NPQ in the dark following challenge with high light: Chr02:65 879 368 ($NPQresidual_{dark}$, RMIP = 0.10) and Chr02:65 900 630 (NPQ_{end}, RMIP = 0.17). These markers are in a region of elevated LD, with the window of genetic markers exhibiting moderate to strong LD ($R^2 \geq 0.25$) with Chr02:65 900 630 encompassing the interval 65 501 078–66 013 031 bp (511 kb), containing 67 annotated gene models (Figure 3a). Significant differences in NPQ_{end} were also observed between sorghum genotypes homozygous for different alleles at Chr02:65 900 630 under LN conditions in 2020 ($P < 0.001$) and under HN conditions in both years ($P = 0.009$ and $P < 0.01$) (Figure 3c). We considered 45 of these as unlikely candidates based on a lack of expression in sorghum leaf tissue; we excluded another 11 gene models with evidence of expression in leaves but lacked functional annotations or had functional annotations inconsistent with a role in the kinetics of NPQ. However, two genes in the mapping interval had plausible functional links to photosynthesis. Another eight genes had functional annotations that, while not strongly linked to photosynthesis or NPQ, were also consistent with a role in NPQ or could not be ruled out.

We reanalyzed previously published maize NPQ kinetics data (Sahay et al., 2023) using a recently published high-density marker set (Grzybowski et al., 2023) to both check for additional evidence, which might support MTA, which was identified for multiple traits but at a "suggestive" rather than "confident" threshold in both cases and, to prioritize candidate genes within the large LD interval present around the Chr02:65 879 368 and Chr02:65 900 630

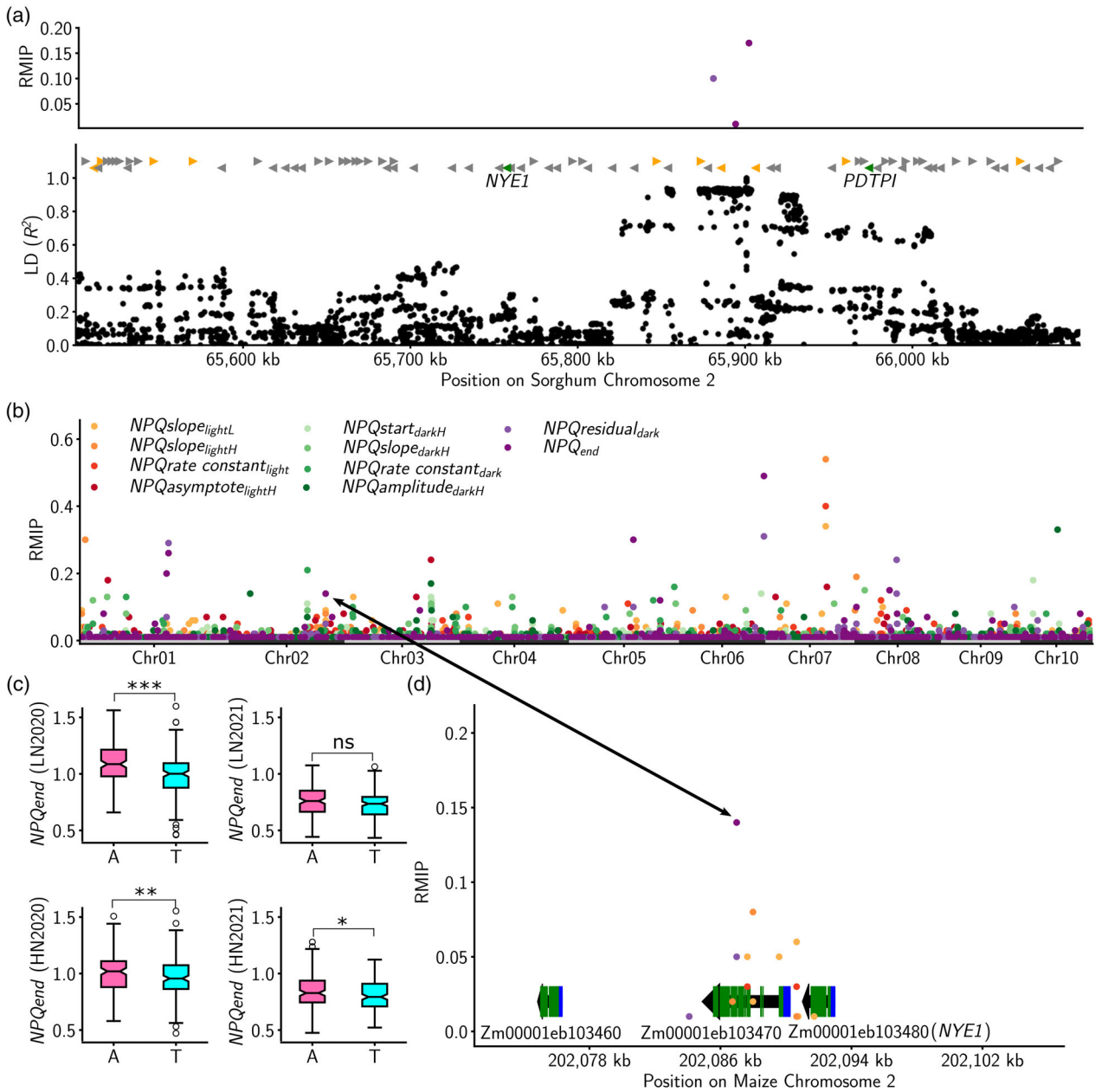

Figure 3. *Non-yellowing 1* (*NYE1*) is associated with variation in NPQ kinetics in sorghum and maize.

(a) Trait-associated SNPs, positions of candidate genes, and linkage disequilibrium (LD) defined mapping interval associated with SNP linked to *NYE1* in Figure 2a and Table S1: 65 500 078 to 66 099 985 bp on chromosome 2. This region contains two SNPs that has RMIP threshold between 0.05 and 0.2, Chr02:65 879 368 ($NPQresidual_{dark}$, RMIP = 0.1) and Chr02:65 900 630 (NPQ_{end}, RMIP = 0.17). The top panel shows traits associated SNPs within this interval (colors correspond to traits given in the legend of Panel b). Triangles indicate the position of annotated sorghum genes within the interval. Gray triangles indicate genes provisionally ruled out as candidates based on annotated function and/or lack of expression in sorghum leaf tissue. Yellow triangles indicate genes that could not be ruled out but lack clear links to chloroplasts, or photosynthesis. Green triangles indicate the position of high-priority candidate genes based on functional annotation. Black dots indicate the LD of SNPs within this mapping interval relative to Chr02:65 879 368.

(b) RMIP results for a reanalysis of published trait data from 746 maize genotypes from the Wisconsin Diversity panel grown in Lincoln, Nebraska, in the summer of 2020 (Sahay et al., 2023) using new higher density genetic markers from resequencing (Grzybowski et al., 2023).

(c) NPQ_{end} values measured under low-nitrogen conditions (LN2020 and LN2021) and high-nitrogen conditions (HN2020 and HN2021) for sorghum genotypes homozygous for either A or T at Chr02:65 900 630. In panel (c) colored boxes indicate the same as in Figure 2d. For each comparison in (c), $n = 153$ sorghum genotypes for the A allele and $n = 170$ sorghum genotypes for the T allele. $^*P < 0.05$, $^{**}P < 0.01$, $^{***}P < 0.001$, n.s., not significant (two-tailed *t*-test).

(d) Zoomed in view of the results from panel (b) for the region from 202 081 to 202 096 kb on maize chromosome 2. Colors of RMIP results correspond to the NPQ kinetics traits labels in panel (b). Zm00001eb103480, the gene labeled in red is one of the two maize co-orthologs of *NYE1*, one of the green colored triangles genes in panel (a). The gene adjacent to *NYE1*, Zm00001eb103470, is orthologous to a sorghum gene considered a high priority candidate gene based on annotated function but a low-priority candidate as it was expressed below 10 TPM in sorghum leaf tissue (Data S4). Data used to produce this figure is given in Data S5.

markers in sorghum. Reanalysis of published maize data identified 14 MTAs with RMIP ≥0.2, while 144 MTAs were identified with RMIP value between the confident (RMIP ≥0.2) and suggestive value (RMIP ≥0.05) (Figure 3b). One of these signals came from a genetic marker on maize chromosome 2 at position 202 086 988, 4.1 kb downstream of Zm00001eb103480. Zm00001eb103480 is one of two maize co-orthologs of Sobic.002G274800, one of the high-priority candidate genes above. Zm00001eb103480 and Sobic.002G274800 are both orthologs of *NYE1* (At4g22920) (Data S4), which encodes a chlorophyll *a* magnesium dechelatase. The 6-kb interval from 202 086 to 202 092 kb on maize chromosome 2 included a cluster of additional MTAs for three different methods of quantifying the rate of NPQ induction under high light: $NPQslope_{lightH}$ (aggregate RMIP = 0.11, three markers), $NPQrate\ constant_{light}$ (aggregate RMIP = 0.06, two markers), and $NPQslope_{lightL}$ (aggregate RMIP = 0.20, six markers) (Figure 3d). These three metrics estimate the rate of NPQ induction from hyperbolic, exponential, and linear functions, respectively. We also identified a statistically significant peak corresponding to the location of Zm00001eb103480 in a conventional mixed-linear-model-based GWAS for $NPQslope_{lightL}$ (Figure S6; Data S5).

Sorghum genotypes differing in their allele for the GWAS hit associated with *NYE1* also differed significantly in their values for $NPQslope_{lightH}$ and NPQ_{end} (Figure 4a,b; Data S1 and S6), consistent with the cluster of GWAS hits for these two traits associated with the maize ortholog of this gene (Figure 3d). Sorghum homozygous for the T allele exhibited significantly slower induction of NPQ ($NPQslope_{lightH}$), lower steady state of NPQ induction ($NPQasymptote_{lightH}$), lower maximum NPQ (NPQ_{max}), and a smaller relaxation of NPQ after 10 min in the dark ($NPQstart_{darkH}$, $NPQamplitude_{darkH}$, and NPQ_{end}) than sorghum homozygous for the A allele (Figure 4a,b). Similarly, maize homozygous for TC allele had significantly lower induction of NPQ under high light conditions ($NPQslope_{lightH}$) than did maize homozygous for the T allele and smaller relaxation after 10 min in the dark (NPQ_{end}) (Figure 4c,d; Data S7). Two *A. thaliana* mutant lines carrying T-DNA insertions in *NYE1* (Figure 4e) exhibited largely consistent phenotypes with each other. Both lines reached lower maximum NPQ values under high light ($NPQasymptote_{lightH}$, NPQ_{max}, and $NPQstart_{darkH}$) and relaxed more slowly in the dark than wild type ($NPQslope_{darkH}$ and $NPQamplitude_{darkH}$ (one of two lines)) ($P \leq 0.04$ for all listed comparisons; Figure 4f–h). Unlike the differences observed between natural variants in sorghum and maize, no statistically significant differences in NPQ_{end} were observed between *nye1* mutants and wild type of *A. thaliana* (Data S8).

The genetic marker linked to *NYE1* was also associated with significant differences in the abundance of photosynthetic pigments. In both greenhouse (178 sorghum genotypes) and field experiments (23 sorghum genotypes) and under both high and low nitrogen treatments, sorghum genotypes homozygous for the T allele at this marker exhibited significantly higher concentrations of chlorophyll *a*, total chlorophyll, and total carotenoids ($P \leq 0.0002$; two-tailed *t*-test, Table 3). While differences were statistically significant under both low and high nitrogen conditions, the differences in the abundance of photosynthetic pigments between sorghum genotypes homozygous for the T or A allele of the *NYE1* linked marker were more pronounced under low nitrogen conditions than high nitrogen conditions (Table 3). Chlorophyll a/b ratios were not significantly different between sorghum plants carrying different alleles of the *NYE1* linked marker under high nitrogen conditions in either the greenhouse or field study. However, in both datasets, significant differences in chlorophyll a/b ratio between sorghum plants carrying different alleles of the *NYE1* linked marker were observed under low nitrogen conditions as a result of greater reductions in chlorophyll a relative in chlorophyll b under low N conditions among sorghum genotypes homozygous for the A allele ($P \leq 0.009$ (greenhouse condition), $P \leq 0.002$ (field condition); two-tailed *t*-test).

Identification of syntenic gene pairs in sorghum and maize

Subsequent to successful mutant validation of the impact of *NYE1* on NPQ kinetics, we conducted a genome-wide search for maize and sorghum gene pairs adjacent to GWAS hits for the same NPQ kinetic phenotypes. We identified 10 maize-sorghum syntenic gene pairs in four genomic intervals that were adjacent to GWAS hits for traits measured as part of this study in 2020 (Figure 5; Data S9). Six of these gene pairs were located in the syntenic interval containing the *NYE1* locus. Two gene pairs were located in a window associated with $NPQstart_{darkH}$ in both maize and sorghum. A single gene pair, encoding a phosphoglucomutase, was associated with the speed of NPQ induction ($NPQslope_{lightL}$) in both species. A single gene pair was associated with $\varphi PSIIamplitude_{darkH}$ and $\varphi PSII_{end}$ in both species (the protocol employed in both this study and the previous maize study also enabled the quantification of the quantum yield of photosystem II (φPSII) (Sahay et al., 2023)). The single most stable identified signal for $\varphi PSIIamplitude_{darkH}$ (RMIP = 0.49) in sorghum was located near Sobic.005G075900, the ortholog of a largely uncharacterized *A. thaliana* gene that is primarily expressed in leaves and encodes a cysteine/histidine-rich C1 domain family protein (At2g16050). The maize ortholog of this sorghum gene, Zm00001eb168930, was also associated with GWAS hits for multiple φPSII kinetic traits and is primarily expressed in mature leaves and roots (Stelpflug et al., 2016).

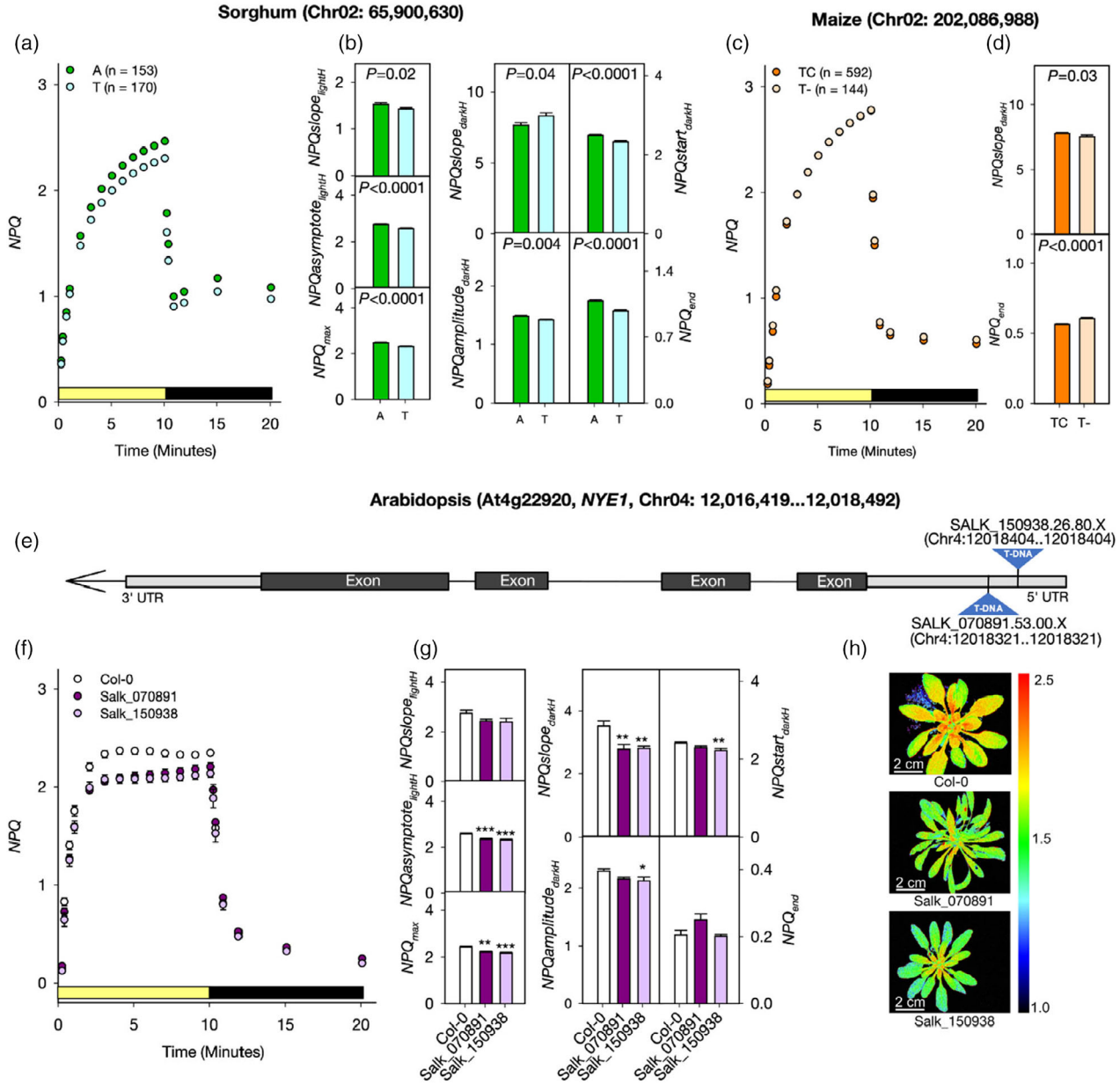

Figure 4. Nonphotochemical quenching (NPQ) phenotypes of *Non-yellowing 1* (*NYE1*) in sorghum, maize, and *A. thaliana*.
(a) Average pattern of NPQ induction and relaxation observed during a 10-min exposure to high-light condition (yellow bar) and relaxation observed during a subsequent 10-min dark treatment (black bar) for sorghum genotypes homozygous either the A or T allele at marker Chr02:65 900 630. Circles indicate median values, and standard error is indicated by vertical lines (too small to be seen behind circles).
(b) Differences in a set of NPQ kinetic traits between sorghum homozygous for different alleles at position Chr02:65 900 630. Height of bars indicate mean values, error bars indicate standard error ($n = 153$ sorghum varieties for A allele and $n = 170$ sorghum varieties for T allele).
(c, d) Average pattern of NPQ kinetics and its traits as described in panel (a), for maize homozygous for either the T- or TC allele of a single base InDeL located at position Chr02:202 086 988. Circles in panel (c) indicate median values, and the standard error is indicated by vertical lines (too small to be seen behind circles). Bars in panel (d) indicate mean values and error bars indicate standard error ($n = 144$ maize varieties for T- allele and $n = 592$ maize varieties for TC allele). In panel (b, d), the *P*-values are the result of a test for significant differences between alleles ($P \leq 0.05$, two-tailed *t*-test).
(e) Structure of the *NYE1* (At4g22920) locus in (*A. thaliana*) and positions of the two T-DNA insertions used in this study. Dark gray boxes indicate protein coding exons. Light gray boxes indicate untranslated regions. The arrow indicates the direction of transcription of *NYE1*.
(f) Pattern of NPQ induction and relaxation kinetics observed for wild type *A. thaliana* (Col-0) and two *nye1* insertion lines (Salk_070891 and Salk_150938).
(g) Differences in a set of NPQ kinetic traits between Col-0 and *nye1* insertion lines. Bars indicate mean values and error bars standard error ($n = 9$ biological replicates for Col-0, $n = 7$ for Salk_070891, $n = 6$ for Salk_150938). Asterisks indicate significant differences between wild type and mutants based on Dunnett's two-way test: $^{*}P \leq 0.05$; $^{**}P \leq 0.01$; $^{***}P \leq 0.001$.
(h) Chlorophyll fluorescence image of NPQ (Scale bar = 2 cm) in Col-0, Salk_070891 and Salk_150938 after 10 min of high light illumination. Data used to produce this figure is given in Data S1, S6, S7 and S8.

Table 3 Quantification of photosynthesis-related pigments measured under high-nitrogen (HN) and low-nitrogen (LN) in greenhouse and field for sorghum genotypes homozygous for either T or A at Chr02:65 900 630

Allele	Chl *a* (μg/ml)	Chl *b* (μg/ml)	Chl *a/b*	Total Chl (μg/ml)	Total Caro (μg/ml)	Total Caro/Chl *a*
	Greenhouse conditions (Seedling stage)					
	HN					
T ($n = 105$)	6.95 ± 0.09	3.72 ± 0.05	1.87 ± 0.02	10.70 ± 0.14	2.86 ± 0.06	0.40 ± 0.008
A ($n = 73$)	5.96 ± 0.13	3.28 ± 0.07	1.81 ± 0.02	9.26 ± 0.20	2.41 ± 0.08	0.39 ± 0.01
Difference	−14.2%	−11.8%	−3.2%	−13.5%	−15.7%	−2.5%
P-value	<**0.0001**	<**0.0001**	0.09	<**0.0001**	<**0.0001**	0.69
	LN					
T ($n = 105$)	5.24 ± 0.14	2.73 ± 0.06	1.92 ± 0.02	7.97 ± 0.20	1.67 ± 0.05	0.29 ± 0.007
A ($n = 73$)	3.99 ± 0.16	2.22 ± 0.07	1.77 ± 0.03	6.23 ± 0.22	1.32 ± 0.06	0.31 ± 0.01
Difference	−23.8%	−18.7%	−7.8%	−21.8%	−20.9%	+6.89%
P-value	< **0.0001**	<**0.0001**	**0.009**	<**0.0001**	**0.0002**	0.42
	Field conditions (Flowering stage)					
	HN2020					
T ($n = 8$)	12.48 ± 0.44	2.75 ± 0.13	4.69 ± 0.18	15.23 ± 0.48	2.78 ± 0.13	4.60 ± 0.11
A ($n = 15$)	10.75 ± 0.26	2.41 ± 0.09	4.58 ± 0.12	13.17 ± 0.31	2.39 ± 0.07	4.54 ± 0.06
Difference	−13.8%	−12.4%	−2.3%	−13.5%	−14%	−1.3%
P-value	<**0.0001**	0.07	0.44	<**0.0001**	<**0.0001**	0.18
	LN2020					
T ($n = 8$)	9.52 ± 0.59	2.10 ± 0.06	4.51 ± 0.15	11.62 ± 0.50	2.15 ± 0.10	4.46 ± 0.10
A ($n = 15$)	7.73 ± 0.26	1.92 ± 0.05	4.06 ± 0.11	9.65 ± 0.30	1.66 ± 0.06	4.71 ± 0.11
Difference	−18.7%	−8.6%	−9.9%	−16.9%	−22.8%	+5.6%
P-value	<**0.0001**	**0.001**	**0.002**	<**0.0001**	<**0.0001**	0.47

P-value represents the difference between alleles in two-tailed *t*-test; numbers in bold are significant ($\alpha = 0.05$); *n* represents number of genotypes.

DISCUSSION

The most stably identified signal in our sorghum NPQ kinetics GWAS under low nitrogen conditions in 2020 was associated with the sorghum ortholog of the *A. thaliana* gene *Suppressor Of Variegation3* (*SVR3*). This genetic variant was not independently discoverable via GWAS in other environments but testing at the single marker level, once the specific SNP was identified, did reveal statistically significant associations with variation in NPQ kinetics across multiple environments. *SVR3* encodes a putative Type A translation elongation factor localized to the chloroplast (Liu et al., 2010). *SVR3* was initially identified as a *suppressor of the variegation2* mutant phenotype. *SVR3* mutant plants exhibit visibly reduced chlorophyll content when grown under control conditions and bleaching in the light when grown at low temperature (Liu et al., 2010). Under control conditions loss-of-function allele of *SVR3* accumulated 75% less photosystem II reaction center protein D1 than wild type plants (Liu et al., 2010). This unbalance in functional PSII centers would lead to an increase in the energy excitation pressure on the remaining functional PSII centers which would, in turn, result in an increase in the need for nonphotochemical dissipation of excitation energy. Ware et al. (2015) showed that in plants with depleted photosystems, NPQ increases. Consistent with this hypothesis, we observed more rapid induction and higher maximum values of NPQ under high-light treatment and slower and less complete relaxation of NPQ in the dark in sorghum genotypes homozygous for the minor allele of the trait-associated SNP linked to the sorghum ortholog of *SVR3* (Figure 2). The observed changes in NPQ kinetics could be explained by a larger pool of the NPQ-related pigments xanthophyll and zeaxanthin, increasing the magnitude of qZ. A piece of evidence consistent with this explanation is that a second allele of *SVR3* was isolated in *A. thaliana* based on resistance to the effects of norflurazon, a blocker of de novo synthesis of carotenoids including xanthophylls (Saini et al., 2011). While *SVR3* defects have only minor effects under control temperatures they may lead to more pronounced changes in chloroplast during stress conditions (Liu et al., 2010). This agrees with our observation in sorghum, where the effect of the genetic marker linked to *SVR3* on NPQ kinetics was statistically significant in multiple years only under nitrogen deficient conditions (Figure 2d).

Another strong candidate gene associated in our study with NPQ kinetics was also linked to chlorophyll metabolism (Figures 2 and 3). A combined GWAS across maize and sorghum identified orthologs in each species of *NYE1* the gene responsible for the segregating cotyledon color phenotype used by Gregor Mendel in determining the laws of genetics (Armstead et al., 2007; Sato et al., 2007). Orthologs of this gene have been cloned in many species, as their loss-of-function mutants frequently exhibit

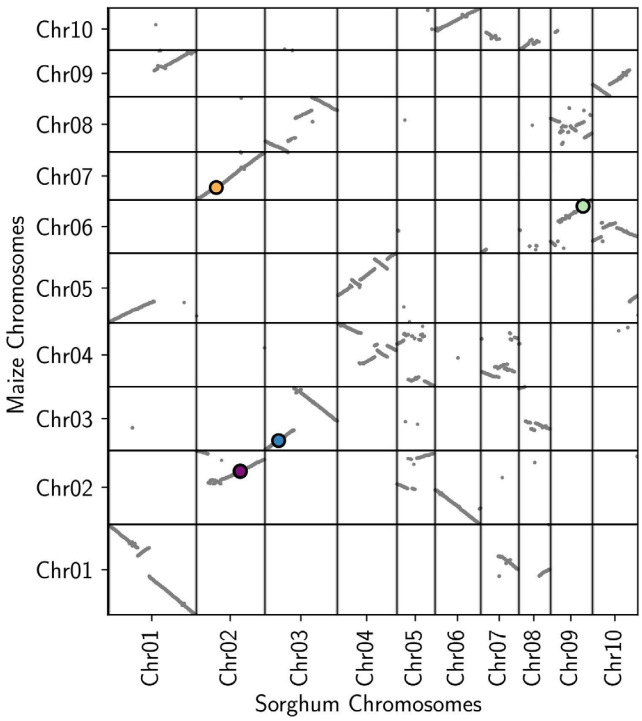

Figure 5. Syntenic GWAS hits for photosynthetic phenotypes identified across maize (2020) and sorghum (LN2020).
The *x*- and *y*-axes indicate annotated gene order along the genomes of sorghum (BTx623 v3) and maize (B73 RefGen v5), respectively. Gray dots mark the locations of maize-sorghum syntenic orthologous gene pairs. Large colored circles with black outlines indicate the positions of syntenic orthologous gene pairs in which the maize gene copy is no more than 100 kb from a GWAS hit for one or more traits identified with an RMIP ≥0.05 ("suggestive") and the sorghum gene copy is no more than 300 kb from a GWAS hit for the same trait or traits identified at the same RMIP ≥0.05 ("suggestive") cutoff. The filled colors of each circle (orange: $NPQslope_{lightL}$, purple: NPQ_{end}, blue: $\varphi PSIIamplitude_{darkH}$, and green: $NPQstart_{darkH}$) indicate the identity of the shared trait between maize and sorghum orthologs. When multiple shared traits were identified, the trait with the greatest average RMIP across the two species was used to select the color shown.

delayed or lack of leaf yellowing during senescence (Armstead et al., 2007; Jiang et al., 2007; Park et al., 2007; Ren et al., 2007). The *Non-yellowing 1* genes encode magnesium-dechelatase, responsible for catalyzing the first committed step of chlorophyll *a* breakdown, the removal of Mg^{+2} from chlorophyll *a* (Shimoda et al., 2016). *NYE1* is highly conserved across plants species consistent with the importance of chlorophyll catabolism for plant survival (Jiao et al., 2020). Possibly to activate chlorophylls catabolism or prevent chlorophyll accumulation, *NYE1* is upregulated during senescence and in response to multiple stresses including low-nitrogen and application of stress hormone of abscisic acid (Park et al., 2007; Ren et al., 2007; Zimmermann et al., 2004). Therefore, we speculate that low nitrogen availability could trigger the catabolism of existing chlorophyll by *NYE1* and the change in chlorophyll *a* to *b* ratio could generate the necessity to adjust the level of photoprotection. In our study, sorghum genotypes differing in their allele for the GWAS hit associated with *NYE1* also differed significantly in their chlorophyll content more strongly at low N than control N conditions (Table 3), which has potential to explain why the effect size and statistical significance of this marker trait association was only sufficiently large to be independently discovered via GWAS in one low nitrogen environment. While both analyzed alleles showed some level of reduction of photosynthesis-related pigments, there were important differences between alleles in relative changes in chlorophylls. In both greenhouse and field conditions, the allelic variance with the stronger reduction in chlorophyll *a* and chlorophyll *a* to *b* ratio under low nitrogen corresponded to the upregulation of NPQ kinetics. The significant reduction in chlorophyll *a* to *b* ratio can lead to excess energy absorption, resulting in the need for upregulation of NPQ kinetics in these genotypes (Figure 4a). The link between NPQ and *NYE1* is further underlined by the fact that in *A. thaliana*, *NYE1* expression is upregulated in NPQ-deficient mutants under high-light conditions while the chlorophyll *a/b* ratio is higher than in wild type (Alboresi et al., 2011). Intriguingly, non-yellowing/stay green is a valuable trait for improving crop stress tolerance and is associated with the domestication of cereals (Thomas & Ougham, 2014). In rice, natural variation in the expression of the *NYE1* ortholog *STAY-GREEN* (*SGR*) is associated with differences in photosynthetic productivity and grain yield (Shin et al., 2020).

At a population level for maize, the initial speed of NPQ induction ($NPQslope_{lightH}$) was only modestly correlated with either the maximum level of NPQ under high light treatment ($NPQasymptote_{lightH}$, $R^2 = 0.01$), or maximum degree of relaxation (NPQ_{end}, $R^2 = 0.04$) (Figure S7). However, the maximum level of NPQ under high-light treatment was substantially correlated with the final degree of NPQ relaxation in the dark ($R^2 = 0.64$), suggesting a potential trade-off between the capacity to adapt to high-light conditions and the ability to optimize photosynthetic productivity under lower light conditions rapidly (Figure S7). Here, we identified individual genetic variants via GWAS for individual traits describing different features of the kinetics of NPQ induction and relaxation. However, in some cases, GWAS hits for multiple NPQ kinetics phenotypes clustered on the sorghum and maize genomes (Figures 2a and 3b). In addition, analysis of the overall pattern of NPQ kinetics in genotypes carrying different alleles of trait-associated markers identified by GWAS (Figures 2c,d and 4a–d) and mutant alleles (Figure 4f,g) suggest that functional variation in a single locus can alter multiple aspects of NPQ kinetics. As a result, it may be necessary to characterize larger numbers of genes to identify a specific genetic intervention or interventions that can alter the kinetics of NPQ in a desired fashion. Fortunately, the consequences of functional variation in orthologous genes appear to be conserved across even distantly related species, as reported previously for five cases in maize and *A. thaliana* (Sahay et al., 2023) and described here for *NYE1* in maize, sorghum, and *A. thaliana*, allowing the results of gene characterization to be shared across different crops and genetic models.

Conservation of phenotypes across orthologous genes has been widely reported among the grasses, including the domestication gene *Shattering1* (Lin et al., 2012) and the flowering time regulator *Heading date1* (Liu et al., 2015). Conservation of function has also been reported in the cloned genes via classical forward genetics as in the case of sorghum *Dwarf 3* (*dw3*) and maize *Brachytic 2* (*br2*), which encode orthologous modulators of polar auxin transport involved in stem elongation (Multani et al., 2003). Maize has served as a genetic model for more than a century, with hundreds of genes subjected to individual investigation and characterization (Schnable & Freeling, 2011). However, forward genetic characterization in sorghum has been more limited (Boyles et al., 2019). GWAS provides an alternative approach to link genes to functions, but the slower decay of LD in the sorghum genome frequently results in mapping intervals that are too large to identify a single candidate gene confidently. This was the case with the GWAS hit identified at Chr02:65 900 630 in this study. The approach we took to identify *NYE1* integrated GWAS results for the same phenotype across maize and sorghum. This approach builds upon prior findings that demonstrated the conservation of a number of flowering time QTLs across maize, sorghum, and foxtail millet (*Setaria italica*) (Mauro-Herrera et al., 2013) and root phenotype associated GWAS hits across maize and sorghum (Zheng et al., 2020). We suspect the approach employed here may also be applicable to other traits and pairs of related species.

EXPERIMENTAL PROCEDURES

Composition and design of sorghum field experiment

The field data presented here were collected from two experiments conducted in the summers of 2020 and 2021 at the University of Nebraska-Lincoln's Havelock Farm. In both years, plots consisted of one 1.52-m row of plants from a single genotype planted with a spacing of 0.76 m between parallel and sequential rows and approximately 7.62 cm spacing between sequential plants in the same row. In both years, no supplemental nitrogen was applied to low-nitrogen (LN) treatment blocks, and a target of 80 pounds of N per acre (89.6 kilograms/hectare) was applied to high-nitrogen (HN) blocks. The 2020 experiment was conducted in a field located at N° 40.861, W° 96.598, and the 2021 experiment was conducted in a field located at N° 40.858, W° 96.596. The 2020 experiment consisted of 347 genotypes drawn from the sorghum association panel plus Tx430 (Casa et al., 2008). A total of four blocks were planted, each consisting of 390 plots with one entry per genotype, plus BTx623 as a repeated check. Two blocks were grown under HN treatment and two under LN treatment. The 2021 experiment consisted of 347 genotypes replicated in two blocks, each consisting of 390 plots, including the replicated check, under LN conditions as in 2020, and 911 sorghum genotypes in two blocks, each consisting of 966 plots including the replicated check under HN. The larger population in HN treatment resulted from the inclusion of sorghum genotypes from the sorghum diversity panel (Griebel et al., 2021) in addition to the previously characterized sorghum association panel lines. The 2020 field experiment was planted on June 8th, and the 2021 field experiment was planted on May 25th. The 2020 field experiment has also been previously described (Grzybowski et al., 2022).

Quantifying NPQ and deriving NPQ kinetics traits

The leaf disks employed for NPQ measurements were collected from the fields between July 29, 2020, and August 5, 2020, and between July 21, 2021, and July 30, 2021, with collection occurring between 16:00 and 18:30 h. Leaf disks were collected and NPQ traits were profiled from leaf disks following the method described previously (Sahay et al., 2023). Briefly, for each plot, three plants were randomly selected for sampling, avoiding edge plants when possible. For each plant, one 0.32-cm^2 leaf disk was collected from the youngest fully expanded leaf, avoiding the midrib. Leaf disks were placed with their adaxial surfaces facing down into 96-well plates, with wet sponges added onto their abaxial surfaces to prevent drying and secure disk position. Plates were inverted (i.e., adaxial face up) and incubated overnight in the dark prior to phenotyping. The following day, plate imaging was performed using a modulated chlorophyll fluorescence imager (FluorCam FC 800-C, Photon Systems Instruments, Drasov, Czech Republic). Leaf disks were subjected to an illumination treatment of 10 min at 2000 $\mu mol\ m^{-2}\ sec^{-1}$ light (1000 $\mu mol\ m^{-2}\ sec^{-1}$ of red-orange light with $\lambda_{max} = 617$ nm and 1000 $\mu mol\ m^{-2}\ sec^{-1}$ of a 6500 K light source) followed by 10 minutes of dark treatment with saturating

flashes of 3200 μmol m^{-2} sec^{-1} (provided by a cool white 6500 K light) for a duration of 800 ms. The minimum (F_o) and maximal (F_m) chlorophyll fluorescence values were measured from the dark-adapted leaves, followed by steady-state fluorescence (F_s) and maximum fluorescence measured under illuminated conditions (F_m') at the following intervals (in seconds): 15, 30, 30, 60, 60, 60, 60, 60, 60, 60, 60, 60, 9, 15, 30, 60, 180, and 300. At each time point, NPQ was estimated via the Stern-Volmer quenching model (Bilger & Björkman, 1994).

$$NPQ = F_m/F_m' - 1$$

The measured NPQ represents the two fastest components: energy-dependent quenching (qE) and modestly slower zeaxanthin-dependent quenching (qZ). NPQ values calculated at each time point were fitted to hyperbola and exponential equations in MATLAB (Matlab R2019b; MathWorks, Natick, MA, USA) to extract parameters reflecting the rate, amplitude, and steady state of the NPQ kinetics curve (Table 1) using the equations described in (Sahay et al., 2023). In both years, plots with no healthy plants present were excluded from sampling and analysis. In 2020, 1550 of 1560 plots were sampled. In 2021 2667 of 2712 plots were sampled.

Data integrity and quality control procedure

Individual leaf disks were subjected to a two-stage quality control and outlier removal process with the first stage based on (F_v/F_m) and goodness of fit for hyperbolic equations fit to the measured NPQ and the second stage based on visual examination of the distribution of each NPQ kinetic trait to identify extreme values. After quality control and outlier removal, data were present for 348 sorghum genotypes in both treatments across both years. Within-year/within-treatment Best Linear Unbiased Estimators (BLUEs) were calculated by fitting a mixed linear model using the *lme4* package (Bates et al., 2015) in R v.4.1.0 (R Core Team, 2020) with the equation $y_i = \mu +$ Genotype$_i$ + Row$_j$ + Block$_k$ + Plate$_l$ + error$_{ijkl}$ where, y_i is the mean trait of interest in the i^{th} genotype planted in the j^{th} row and k^{th} block, and placed in l^{th} 96-well plate during NPQ quantification, μ is the overall mean of the population, Genotype$_i$ is fixed effect of genotype *i*, *Row*$_j$ is random effect of row *j*, Block$_k$ is random effect of block *j*, Plate$_l$ is random effect of 96-well plate *l*, and error$_{ijkl}$ is the residual. Visual examination of BLUE distributions identified nine sorghum genotypes (~2.6% of the total population) with extreme values for one or more NPQ traits. BLUEs for 339 sorghum genotypes were employed for genome-wide association studies.

The variance explained by individual factors within the model was used to estimate within-year/within-treatment heritability using the following equation: ($H^2 = \sigma_G^2 \,/\, (\sigma_G^2 + \sigma_e^2/r)$) where σ_G^2 was the total variance explained by the genotype factor in each mixed linear model and σ_e^2/r is the total residual variance in each mixed linear model divided by the number of replicates of each genotype within the same treatment and year.

Quantitative genetic analyses

A published set of 43 million segregating single nucleotide polymorphisms (SNPs), structural variants, and insertion/deletions (InDels) derived from whole–genome resequencing of the sorghum association panel (Boatwright et al., 2022) was filtered using VCFtools v.0.1 (Danecek et al., 2011) and bcftools v.1.17 (Danecek et al., 2021) retaining only biallelic SNP markers with a minor allele frequency (MAF) >0.05 and a frequency of heterozygous genotype calls <0.05 among the final set of 339 sorghum genotypes. These filtering criteria produced a final set of 4 457 229 SNP markers.

Marker–trait associations in sorghum were considered confident when identified in at least 20 of 100 resampling analyses (RMIP ≥0.2), and suggestive when identified in at least 5–19 out of 100 resampling analyses (RMIP ≥0.05) conducted with FarmCPU as implemented in rMVP (Liu et al., 2016; Yin et al., 2021). In each iteration, a random 10% of sorghum genotypes were masked, and a separate FarmCPU analysis was conducted, keeping the set of markers significantly above a threshold of 5.107×10^{-8}. The significance threshold employed corresponds to 0.05 divided by the approximately 978 957 effective/independent number of markers in the filtered biallelic SNP dataset as estimated by GEC v.0.2 (Li et al., 2012).

Marker-trait association in maize was conducted using a published set of maize NPQ kinetics phenotypes (Sahay et al., 2023). FarmCPU resampling as described above and mixed linear model based GWAS (Yu et al., 2006) was conducted with a set of 16 634 049 markers representing the subset of the 46 million high confidence markers identified previously (Grzybowski et al., 2023) with a minor allele frequency >5% and significant threshold 3×10^{-9}.

Linkage disequilibrium (LD) calculations were performed using plink v1.90; (Purcell, 2012). Windows of interest were defined by first calculating LD between the marker identified by FarmCPU resampling and all SNPs within an interval of approximately 10 Mb and then identifying the first and last SNPs within the interval that exhibited linkage disequilibrium with the GWAS hit above the cutoff used to define the window.

Quantification of photosynthesis-related pigments

Leaf samples were collected from field and greenhouse-grown plants under high and low N conditions for the analysis of photosynthetic pigments. In the greenhouse experiment, seeds were surface sterilized with 20% bleach for 20 min, followed by five times washing, and overnight soaking in distilled water. Seeds were sown in 3.5 inch ×3.5 inch pots (SQN03500B66, Hummert International, Earth City, MO, USA) filled with potting mix (20% MitroMix200, 30% sterilized sand and 50% fine vermiculite) with 14/10 h photoperiod at 29/22°C day/night temperature. Beginning 4 days after germination, seedlings were irrigated with either Hoagland media containing 210.2 mg of N L^{-1} (high nitrogen), or Hoagland media with reduced nitrogen content of 105.1 mg of N L^{-1} (low nitrogen). Four leaf disks (0.25 cm^2) per genotype per treatment were harvested from when plants were 21 days post-germination. Leaf disks were collected into 500 μl of pre-chilled 90% methanol (A452-1, Fisher Scientific, Hampton, NH, USA), vortexed and finally incubated in the dark for 4 days at 4°C. Supernatant was collected and the leaf disks were washed with additional methanol by centrifuge for 2 min at 1902 × g at 4°C (5424R, Eppendrof, Enfield, CT, USA). Supernatant was transferred to 96-well plates to measure the absorbance at 470, 652 and 665 nm using a plate reader (Microplate Reader HT, Bio Tek, Winooski, VT, USA). Chlorophyll (Chl) *a*, *b* and total carotenoid contents were determined using the measured absorptions and the equations of (Lichtenthaler, 1987). Leaf disks from field-grown plants were collected in the 2020 sorghum field experiment approximately 65 days after planting following the same sampling and treatment protocol described for the greenhouse experiment.

Quantification of NPQ in *nye1* mutants

The seeds of *A. thaliana* T-DNA insertion *nye1* mutants (Salk_070891 and Salk_150938) and the corresponding Columbia (Col-0) wild type control (CS60000) were obtained from the Arabidopsis Biological Resource Center (ABRC) at Ohio State University

(Alonso et al., 2003). Lines were selfed and homozygous progeny was obtained. Homozygosity for *nye1* mutant plants was confirmed by PCR using the T-DNA-specific primer LBb1.3 and gene-specific left primer and right primer for Salk_070891 and Salk_150938 lines (Table S2) which were designed using the Salk T-DNA primer design tool (http://signal.Salk.edu/tdnaprimers.2.html). The RT-PCR was used to confirm that *nye1* mutants abolished expression of the mature *NYE1* transcript (Figure S8). The primers sequences used for RT-PCR were designed using Integrated DNA technologies tool (http://www.idtdna.com) and presented in Table S2. The seeds of homozygous T-DNA mutant lines and their corresponding wild type were stratified at 4°C for 4 days in the dark, sown in 3.5 inch × 3.5 inch (8.89 × 8.89 centimeter) pots (SQN03500B66, Hummert International, Earth City, MO, USA) filled with soil-less potting mix (1 220 338; BM2 Germination and Propagation Mix; Berger, SaintModeste, Canada) at 21°C day/18°C night with a 10-h-light/14-h-dark photoperiod (200 μmol m^{-2} sec^{-1}) and 60% relative humidity in a reach-in growth chamber (AR-66 L2; Percival, Perry, IA, USA). One week after germination, seedlings were thinned to one per pot; plants were watered three times a week with 150 ppm liquid fertilizer (Peter's 201020 general purpose fertilizer, 25#, Peters Inc., Allentown, PA, USA). Plants were repositioned three times a week at random locations in the chamber.

NPQ kinetics were measured and parameterized as above, except with a few modifications described below. Four-week-old whole plants were imaged after 20 minutes of dark adaptation, with saturating pulses of 2400 μmol m^{-2} sec^{-1} and actinic light of 1000 μmol m^{-2} sec^{-1} (a combination of 500 μmol m^{-2} sec^{-1} of a red-orange light with $\lambda_{max} = 617$ nm and 500 μmol m^{-2} sec^{-1} of a cool white 6500 K light) were used. An area of 270–280 pixels was chosen manually from a portion of three of the youngest, fully expanded leaves facing the uniform illumination and used for NPQ quantification and analysis.

Comparative GWAS analysis

The coding sequences of annotated maize genes from B73 RefGen_V5 (Hufford et al., 2021) and annotated sorghum genes from the BTx623 V3 (McCormick et al., 2018) reference genomes were downloaded from Phytozome, selecting the "primaryTranscriptOnly" files for each species (Goodstein et al., 2012). Syntenic orthologs were identified by (1) identifying genes with similar coding sequences between the two species using LASTZ with a seed of match12, a minimum identity of 70% and minimum coverage of 50% (Harris, 2007), (2) identifying syntenic blocks of homologous genes using QuotaAlign with a quota of 1:2 for sorghum: maize (Tang et al., 2011), reflecting the whole-genome duplication that occurred in maize after the split of the maize and sorghum lineages; and (3) polishing the raw QuotaAlign gene pairs via the Zhang et al. method (Zhang et al., 2017).

Statistical data of insertion mutant phenotypes

Statistical analysis of NPQ kinetics measurements in mutants was performed using SAS (version 9.4, SAS Institute Inc., Cary, NC, USA). Normality of distributions was evaluated using the Shapiro–Wilk test and the homogeneity of variance in data was evaluated using the Brown–Forsythe method. When the assumption of either normality or homogeneity of variance were violated as determined by the above methods, data were log-transformed prior to testing for significant differences between genotypes. To evaluate potential differences between alternative alleles the two-tailed *t*-tests were performed ($\alpha = 0.05$). To evaluate potential differences between mutant and wild type plants, one-way ANOVAs ($\alpha = 0.05$) were performed followed by Dunnett's test to address the multiple comparison problem of multiple insertion lines being compared to a common wild type control.

AUTHOR CONTRIBUTIONS

JCS, MG, and KG conceived the project. SS collected the data. SS, NS, and MG analyzed the data. HMS and RVM conducted additional analyses. SS, NS, JCS, and KG designed figures and drafted the manuscript. MG designed additional figures. All authors read, edited, and approved the final manuscript.

ACKNOWLEDGMENTS

The authors thank Mackenzie Zwiener, Brandi Sigmon, and Christine Smith for their leadership on field design and field experiment execution in 2020 and 2021. The authors thank Aldi Airori, Grace Carey, Sierra Conway, Elijah Frost, Remy Hirwa, Alliance Igiraneza, Luke Micek, Prince Ngiruwonsanga, Nathaniel Pester, Isabel Sigmon, Isaac Stevens, Lou Townsend, Daniella Norah Tumusiine, and Leighton Wheeler, for assistance with planting, field maintenance, and field data collection. The authors thank Guangchao Sun and Aime V. Nishimwe for their efforts designing and conducting sorghum greenhouse experiments. The authors thank Annie Nelson for assistance in plate imaging and Eleanor Browne, Quinton Browne, Rachel Gerdes, Eleana Kang, Quinn Kimbell, Ryenne Leising, Bailey McClean, Pascaline Nyonshuti, and Hayley Ramirez for assistance in the collection of plant materials from the field. The authors thank Harshita Mangal for assistance in the analysis of data. This project was supported by the U.S. Department of Energy, Grants no. DE-SC0020355 and DE-SC0023138, the National Science Foundation under grant OIA-1826781, USDA NIFA under the AI Institute: for Resilient Agriculture, Award No. 2021–67021-35329 and the Foundation for Food and Agriculture Research Award No. 602757 to JCS. This project was supported by the National Science Foundation under awards OIA-1557417 (CRRI and ESCoR FIRST) and IOS-2142993 (CAREER) and the University of Nebraska Lincoln under a Laymen award to KG. HMD was supported by a FAPESP award, (support # 2022/16208–9).

CONFLICT OF INTEREST STATEMENT

James C. Schnable has equity interests in Data2Bio, LLC; Dryland Genetics LLC; and EnGeniousAg LLC. He is a member of the scientific advisory board of GeneSeek and currently serves as a guest editor for The Plant Cell. The authors declare no other competing interests.

DATA AVAILABILITY STATEMENT

NPQ data collected from sorghum are provided as Supplementary Data Sets associated with this paper. Raw measurements of NPQ parameters for each leaf disk at each time point are provided for individual leaf disks (Data S1). Within year-within treatment BLUEs for NPQ kinetic phenotypes are provided as Data S2. The genetic marker data employed in this study has been previously published (Boatwright et al., 2022; Grzybowski et al., 2023). The sorghum genetic marker data is available from the European Variant Archive (PRJEB51985) and the maize genetic

marker data is available from Dryad: https://doi.org/10.5061/dryad.bnzs7h4f1. The set of FarmCPU GWAS hits identified for all traits described in this study for sorghum are provided as Data S3. Annotated sorghum genes within the mapping interval for each GWAS hit presented in Table S1 are provided in Data S4. The set of FarmCPU GWAS hits identified in maize using resequenced marker data are provided as Data S5. Data of genotype calls across the sorghum association panel for representative GWAS hits (Data S6) and across the Wisconsin Diversity maize panel for GWAS hit corresponding to *NYE1* (Data S7) are provided. Raw data of NPQ values for *A. thaliana* mutants are provided as Data S8.

SUPPORTING INFORMATION

Additional Supporting Information may be found in the online version of this article.

Figure S1. Diversity of nonphotochemical quenching induction and relaxation patterns observed in the sorghum association panel.

Figure S2. Distributions of nonphotochemical quenching traits across years and treatments.

Figure S3. Correlations of nonphotochemical quenching kinetics traits presented in Figure 1 across years and treatments.

Figure S4. Results of genome-wide association study for nonphotochemical quenching kinetic traits measured for sorghum genotypes in two treatments over 2 years.

Figure S5. Zoomed in view of the Sobic.004G128900/*SVR3* candidate gene and LD window.

Figure S6. Conventional Mixed-Linear-Model-based genome-wide association study identifies signals at the genomic interval corresponding to Zm00001eb10348 (*NYE1*).

Figure S7. Correlation among hyperbola derived nonphotochemical quenching traits in maize.

Figure S8. Molecular verification of *Nye1* mutants.

Table S1. Locations and mapping intervals for significant genome-wide association study hits associated with nonphotochemical quenching relaxation in dark traits under low nitrogen treatment in 2020.

Table S2. Names and sequences of primers used for PCR to verify homozygosity (1) and for RT-PCR to verify the absence of mature mRNA (2) of *Arabidopsis thaliana* mutants in *NYE1* (At4g22920) gene.

Data S1. NPQ and φPSII values at each time point during light and dark treatments for each sorghum leaf disk collected in 2020 and 2021.

Data S2. BLUE values for each sorghum genotype in 2020 and 2021 under HN and LN treatments.

Data S3. Results of resampling-based genome-wide association study in sorghum. Includes analyses conducted in both HN and LN treatments in 2020 and 2021.

Data S4. Set of annotated sorghum genes present within the mapping intervals for each GWAS hit described in Table S1.

Data S5. Results of resampling-based genome-wide association study in maize conducted using new higher density marker data. Includes results of separate analyses conducted using published trait data from 2020 and 2021.

Data S6. Genotype calls across the sorghum association panel for trait-associated markers described in Table S1. Heterozygous calls were converted to missing data.

Data S7. Genotype calls across the Wisconsin Diversity maize panel for Chr2:2286988 allele information for genome-wide association study hit corresponding to *NYE1* in maize.

Data S8. Nonphotochemical quenching values at each time point during light and dark treatment for each wild type and *nye1* plant for which data is reported in Figure 4.

Data S9. Ten maize-sorghum syntenic gene pairs in four genomic intervals that were adjacent to genome-wide association study hits for traits measured.

REFERENCES

Alboresi, A., Dall'Osto, L., Aprile, A., Carillo, P., Roncaglia, E., Cattivelli, L. *et al.* (2011) Reactive oxygen species and transcript analysis upon excess light treatment in wild-type *Arabidopsis thaliana* vs a photosensitive mutant lacking zeaxanthin and lutein. *BMC Plant Biology*, **11**, 1–22.

Alonso, J.M., Stepanova, A.N., Leisse, T.J., Kim, C.J., Chen, H., Shinn, P. *et al.* (2003) Genome-wide insertional mutagenesis of *Arabidopsis thaliana*. *Science*, **301**(5633), 653–657.

Armstead, I., Donnison, I., Aubry, S., Harper, J., Hoortensteiner, S., James, C. *et al.* (2007) Cross-species identification of Mendel's I locus. *Science*, **315**(5808), 73.

Bates, D., Mächler, M., Bolker, B. & Walker, S. (2015) Fitting linear mixed-effects models using *lme4*. *Journal of Statistical Software*, **67**(1), 1–48.

Bilger, W. & Björkman, O. (1994) Relationships among violaxanthin deepoxidation, thylakoid membrane conformation, and nonphotochemical chlorophyll fluorescence quenching in leaves of cotton (*Gossypium hirsutum L.*). *Planta*, **193**, 238–246.

Boatwright, J.L., Sapkota, S., Jin, H., Schnable, J.C., Brenton, Z., Boyles, R. *et al.* (2022) Sorghum association panel whole-genome sequencing establishes cornerstone resource for dissecting genomic diversity. *The Plant Journal*, **111**(3), 888–904.

Boyles, R.E., Brenton, Z.W. & Kresovich, S. (2019) Genetic and genomic resources of sorghum to connect genotype with phenotype in contrasting environments. *The Plant Journal*, **97**(1), 19–39.

Burgess, A.J., Retkute, R., Preston, S.P., Jensen, O.E., Pound, M.P., Pridmore, T.P. *et al.* (2016) The 4-dimensional plant: effects of wind-induced canopy movement on light fluctuations and photosynthesis. *Frontiers in Plant Science*, **7**, 1392.

Casa, A.M., Pressoir, G., Brown, P.J., Mitchell, S.E., Rooney, W.L., Tuinstra, M.R. *et al.* (2008) Community resources and strategies for association mapping in sorghum. *Crop Science*, **48**(1), 30–40.

Danecek, P., Auton, A., Abecasis, G., Albers, C.A., Banks, E., DePristo, M.A. *et al.* (2011) The variant call format and VCFtools. *Bioinformatics*, **27**(15), 2156–2158.

Danecek, P., Bonfield, J.K., Liddle, J., Marshall, J., Ohan, V., Pollard, M.O. *et al.* (2021) Twelve years of SAMtools and BCFtools. *GigaScience*, **10**(2), giab008.

De Souza, A.P., Burgess, S.J., Doran, L., Hansen, J., Manukyan, L., Maryn, N. *et al.* (2022) Soybean photosynthesis and crop yield are improved by accelerating recovery from photoprotection. *Science*, **377**(6608), 851–854.

Gamba, D., Lorts, C., Haile, A., Sahay, S., Lopez, L., Xia, T. *et al.* (2022) The genomics and physiology of abiotic stressors associated with global elevation gradients in *Arabidopsis thaliana*. *bioRxiv*, 2022.

Goodstein, D.M., Shu, S., Howson, R., Neupane, R., Hayes, R.D., Fazo, J. *et al.* (2012) Phytozome: a comparative platform for green plant genomics. *Nucleic Acids Research*, **40**(D1), D1178–D1186.

Griebel, S., Adedayo, A. & Tuinstra, M.R. (2021) Genetic diversity for starch quality and alkali spreading value in sorghum. *The Plant Genome*, **14**(1), e20067.

Grzybowski, M.W., Mural, R.V., Xu, G., Turkus, J., Yang, J. & Schnable, J.C. (2023) A common resequencing-based genetic marker data set for global maize diversity. *The Plant Journal*, **113**(6), 1109–1121.

Grzybowski, M.W., Zwiener, M., Jin, H., Wijewardane, N.K., Atefi, A., Naldrett, M.J. *et al.* (2022) Variation in morpho-physiological and metabolic responses to low nitrogen stress across the sorghum association panel. *BMC Plant Bology*, **22**(1), 1–14.

Harris, R.S. (2007) *Improved pairwise alignment of genomic DNA*. PhD thesis, Pennsylvania State University.

Herritt, M., Dhanapal, A.P. & **Fritschi, F.B.** (2016) Identidication of genomic loci associated with the photochemical reflectance index by genome-wide association study in soybean. *The Plant Genome*, **9**(2), plantgenome2015-08.

Hufford, M.B., Seetharam, A.S., Woodhouse, M.R., Chougule, K.M., Ou, S., Liu, J. ***et al.*** (2021) De novo assembly, annotation, and comparative analysis of 26 diverse maize genomes. *Science*, **373**(6555), 655–662.

Jiang, H., Li, M., Liang, N., Yan, H., Wei, Y., Xu, X. ***et al.*** (2007) Molecular cloning and function analysis of the stay green gene in rice. *The Plant Journal*, **52**(2), 197–209.

Jiao, B., Meng, Q. & **Lv, W.** (2020) Roles of stay-green (sgr) homologs during chlorophyll degradation in green plants. *Botanical Studies*, **61**(1), 1–9.

Jung, H.S. & **Niyogi, K.K.** (2009) Quantitative genetic analysis of thermal dissipation in Arabidopsis. *Plant Physiology*, **150**(2), 977–986.

Kaiser, E., Morales, A. & **Harbinson, J.** (2018) Fluctuating light takes crop photosynthesis on a rollercoaster ride. *Plant Physiology*, **176**(2), 977–989.

Kromdijk, J., Głowacka, K., Leonelli, L., Gabilly, S.T., Iwai, M., Niyogi, K.K. ***et al.*** (2016) Improving photosynthesis and crop productivity by accelerating recovery from photoprotection. *Science*, **354**(6314), 857–861.

Li, M.X., Yeung, J.M., Cherny, S.S. & **Sham, P.C.** (2012) Evaluating the effective numbers of independent tests and significant p-value thresholds in commercial genotyping arrays and public imputation reference datasets. *Human Genetics*, **131**, 747–756.

Li, X.P., BjoÈrkman, O., Shih, C., Grossman, A.R., Rosenquist, M., Jansson, S. ***et al.*** (2000) A pigment-binding protein essential for regulation of photosynthetic light harvesting. *Nature*, **403**(6768), 391–395.

Lichtenthaler, H.K. (1987) Chlorophylls and carotenoids: pigments of photosynthetic biomembranes. *Methods in Enzymology*, **148**, 350–382.

Lin, Z., Li, X., Shannon, L.M., Yeh, C.T., Wang, M.L., Bai, G. ***et al.*** (2012) Parallel domestication of the *Shattering1* genes in cereals. *Nature Genetics*, **44**(6), 720–724.

Liu, H., Liu, H., Zhou, L., Zhang, Z., Zhang, X., Wang, M. ***et al.*** (2015) Parallel domestication of the *heading date 1* gene in cereals. *Molecular Biology and Evolution*, **32**(10), 2726–2737.

Liu, X., Huang, M., Fan, B., Buckler, E.S. & **Zhang, Z.** (2016) Iterative usage of fixed and random effect models for powerful and efficient genome-wide association studies. *PLoS Genetics*, **12**(2), e1005767.

Liu, X., Rodermel, S.R. & **Yu, F.** (2010) A *var2* leaf variegation SUPPRESSOR locus, *SUPPRESSOR OF VARIEGATION3*, encodes a putative chloroplast translation elongation factor that is important for chloroplast development in the cold. *BMC Plant Biology*, **10**(1), 1–18.

Mauro-Herrera, M., Wang, X., Barbier, H., Brutnell, T.P., Devos, K.M. & **Doust, A.N.** (2013) Genetic control and comparative genomic analysis of flowering time in *Setaria* (*Poaceae*). *G3: Genes, Genomes, Genetics*, **3**(2), 283–295.

McCormick, R.F., Truong, S.K., Sreedasyam, A., Jenkins, J., Shu, S., Sims, D. ***et al.*** (2018) The *Sorghum bicolor* reference genome: improved assembly, gene annotations, a transcriptome atlas, and signatures of genome organization. *The Plant Journal*, **93**(2), 338–354.

Muller, P., Li, X.P. & **Niyogi, K.K.** (2001) Non-photochemical quenching. A response to excess light energy. *Plant Physiology*, **125**(4), 1558–1566.

Multani, D.S., Briggs, S.P., Chamberlin, M.A., Blakeslee, J.J., Murphy, A.S. & **Johal, G.S.** (2003) Loss of an MDR transporter in compact stalks of maize *br2* and sorghum *dw3* mutants. *Science*, **302**(5642), 81–84.

Mural, R.V., Grzybowski, M., Miao, C., Damke, A., Sapkota, S., Boyles, R.E. ***et al.*** (2021) Meta-analysis identifies pleiotropic loci controlling phenotypic trade-offs in sorghum. *Genetics*, **218**(3), iyab087.

Niyogi, K.K., Grossman, A.R. & **Björkman, O.** (1998) Arabidopsis mutants define a central role for the xanthophyll cycle in the regulation of photosynthetic energy conversion. *The Plant Cell*, **10**(7), 1121–1134.

Park, S.Y., Yu, J.W., Park, J.S., Li, J., Yoo, S.C., Lee, N.Y. ***et al.*** (2007) The senescence-induced staygreen protein regulates chlorophyll degradation. *The Plant Cell*, **19**(5), 1649–1664.

Pearcy, R.W. (1990) Sunflecks and photosynthesis in plant canopies. *Annual Review of Plant Biology*, **41**(1), 421–453.

Purcell, S. (2012) Plink (1.07) documentation.

R Core Team. (2020) *R: A Language and Environment for Statistical Computing*. Vienna, Austria: R Foundation for Statistical Computing. https://www.R-project.org/

Ren, G., An, K., Liao, Y., Zhou, X., Cao, Y., Zhao, H. ***et al.*** (2007) Identification of a novel chloroplast protein *AtNYE1* regulating chlorophyll degradation during leaf senescence in Arabidopsis. *Plant Physiology*, **144**(3), 1429–1441.

Rungrat, T., Almonte, A.A., Cheng, R., Gollan, P.J., Stuart, T., Aro, E.M. ***et al.*** (2019) A genome-wide association study of non- photochemical quenching in response to local seasonal climates in *Arabidopsis thaliana*. *Plant Direct*, **3**(5), e00138.

Sahay, S., Grzybowski, M., Schnable, J.C. & **Głowacka, K.** (2023) Genetic control of photoprotection and photosystem ii operating efficiency in plants. *New Phytologist*, **239**, 1068–1082.

Saini, G., Meskauskiene, R., Pijacka, W., Roszak, P., Sjögren, L.L., Clarke, A.K. ***et al.*** (2011) Happy on norflurazon (hon) mutations implicate perturbance of plastid homeostasis with activating stress acclimatization and changing nuclear gene expression in norflurazon-treated seedlings. *The Plant Journal*, **65**(5), 690–702.

Sato, Y., Morita, R., Nishimura, M., Yamaguchi, H. & **Kusaba, M.** (2007) Mendel's green cotyledon gene encodes a positive regulator of the chlorophyll-degrading pathway. *Proceedings of the National Academy of Sciences*, **104**(35), 14169–14174.

Schnable, J.C. & **Freeling, M.** (2011) Genes identified by visible mutant phenotypes show increased bias toward one of two subgenomes of maize. *PLoS One*, **6**(3), e17855.

Shimoda, Y., Ito, H. & **Tanaka, A.** (2016) Arabidopsis STAY-GREEN, Mendel's green cotyledon gene, encodes magnesium-dechelatase. *The Plant Cell*, **28**(9), 2147–2160.

Shin, D., Lee, S., Kim, T.H., Lee, J.H., Park, J., Lee, J. ***et al.*** (2020) Natural variations at the stay-green gene promoter control lifespan and yield in rice cultivars. *Nature Communications*, **11**(1), 2819.

Stelpflug, S.C., Sekhon, R.S., Vaillancourt, B., Hirsch, C.N., Buell, C.R., de Leon, N. ***et al.*** (2016) An expanded maize gene expression atlas based on RNA sequencing and its use to explore root development. *The Plant Genome*, **9**(1), 1–16.

Tang, H., Lyons, E., Pedersen, B., Schnable, J.C., Paterson, A.H. & **Freeling, M.** (2011) Screening synteny blocks in pairwise genome comparisons through integer programming. *BMC Bioinformatics*, **12**(1), 1–11.

Tang, Y.H., Washitani, I., Tsuchiya, T. & **Iwaki, H.** (1988) Fluctuation of photosynthetic photon flux density within a *Miscanthus sinensis* canopy. *Ecological Research*, **3**(3), 253–266.

Thomas, H. & **Ougham, H.** (2014) The stay-green trait. *Journal of Experimental Botany*, **65**(14), 3889–3900.

Wang, Q., Zhao, H., Jiang, J., Xu, J., Xie, W., Fu, X. ***et al.*** (2017) Genetic architecture of natural variation in rice nonphotochemical quenching capacity revealed by genome-wide association study. *Frontiers in Plant Science*, **8**, 1773.

Ware, M.A., Giovagnetti, V., Belgio, E. & **Ruban, A.V.** (2015) Psbs protein modulates non-photochemical chlorophyll fluorescence quenching in membranes depleted of photosystems. *Journal of Photochemistry and Photobiology, B: Biology*, **152**, 301–307.

Wei, Y., Liu, S., Xiong, D., Xiong, Z., Zhang, Z., Wang, F. ***et al.*** (2022) Genome- wide association study for non-photochemical quenching traits in *Oryza sativa* L. *Agronomy*, **12**(12), 3216.

Yin, L., Zhang, H., Tang, Z., Xu, J., Yin, D., Zhang, Z. ***et al.*** (2021) rMVP: a memory-efficient, visualization-enhanced, and parallel-accelerated tool for genome-wide association study. *Genomics, Proteomics & Bioinformatics*, **19**(4), 619–628.

Yu, J., Pressoir, G., Briggs, W.H., Vroh Bi, I., Yamasaki, M., Doebley, J.F. ***et al.*** (2006) A unified mixed-model method for association mapping that accounts for multiple levels of relatedness. *Nature Genetics*, **38**(2), 203–208.

Zhang, Y., Ngu, D.W., Carvalho, D., Liang, Z., Qiu, Y., Roston, R.L. ***et al.*** (2017) Differentially regulated orthologs in sorghum and the subgenomes of maize. *The Plant Cell*, **29**(8), 1938–1951.

Zheng, Z., Hey, S., Jubery, T., Liu, H., Yang, Y., Coffey, L. ***et al.*** (2020) Shared genetic control of root system architecture between *Zea mays* and *Sorghum bicolor*. *Plant Physiology*, **182**(2), 977–991.

Zhu, X.G., Ort, D.R., Whitmarsh, J. & **Long, S.P.** (2004) The slow reversibility of photosystem ii thermal energy dissipation on transfer from high to low light may cause large losses in carbon gain by crop canopies: a theoretical analysis. *Journal of Experimental Botany*, **55**(400), 1167–1175.

Zimmermann, P., Hirsch-Hoffmann, M., Hennig, L. & **Gruissem, W.** (2004) GENEVESTIGATOR. Arabidopsis microarray database and analysis toolbox. *Plant Physiology*, **136**(1), 2621–2632.